

Electron microscopy

Electron microscopy and immunoelectron microscopy were performed as described^{29,30}. For electron microscopy, cell samples were fixed in 1.5% glutaraldehyde for 2 h. For immunoelectron microscopy, cells were fixed with 0.1% glutaraldehyde for 10 min.

Reverse transcription-polymerase chain reaction (RT-PCR)

After four days culture of Flk1⁺ cells with 10% FCS, cells (Fig. 1b) were used as a source of SMA⁺ RNA. Total RNA was prepared with TRIzol reagent (Life Technologies, Inc.), reverse transcribed by oligo (dT) priming and PowerScript-Reverse Transcriptase (CLONTECH Laboratories), and PCR was performed with the following primers: SMA forward: 5'-ACGGCCGCTCCTCTTCTC-3', reverse 5'-GCCAGCTTCGTCGATTCC-3', smooth muscle myosin heavy chain forward: 5'-GACAACTCTCTCGCTTTGG-3', reverse: 5'-GCTCTCCAAAAGCAGGTAC-3', h1-calponin forward: 5'-GATACGAATTCAGAGG TGCAGACGGAGGCTC-3', reverse: 5'-GATACAAGCTTTCAATCCACTCTCTCAG CTCC-3', SM22 α forward: 5'-GCAGTCCAAAATTGAGAAGA-3', reverse: 5'-CTGTTGCTGCCCATTTGAAG-3'.

Chick/mouse chimaeric assay

CCE/nLacZ cells were generated by cotransfection of elongation factor 1 promoter-driven LacZ gene with nuclear localization signal (T. Kunisada) and murine phosphoglycerate kinase 1 promoter-driven puromycin resistant gene constructs and selection by 2 μ g ml⁻¹ puromycin. We injected 1–2 \times 10⁶ Flk1⁺ cells in 2–4 μ l of phosphate buffered saline (PBS) into hearts of stage 16–17 chick embryos with glass needles. Embryos were killed 2–3 days after injection and fixed with 2% paraformaldehyde at 4 °C for 10 min. A X-gal analogue, magenta gal (Nakarai), was used as substrate for whole-mount staining; stained embryos were frozen in OCT, cryosectioned at 6–7 μ m and stained for PECAM1 or SMA. PECAM1 staining was performed using TSA Indirect, tyramide signal amplification reagent (NEN Life Science Products).

Received 26 June; accepted 23 August 2000.

- Suri, C. *et al.* Requisite role of angiopoietin-1, a ligand for the TIE2 receptor, during embryonic angiogenesis. *Cell* **87**, 1171–1180 (1996).
- Folkman, J. & D'Amore, P. A. Blood vessel formation: What is its molecular basis? *Cell* **87**, 1153–1155 (1996).
- Darland, D. C. & D'Amore, P. A. Blood vessel maturation: vascular development comes of age. *J. Clin. Invest.* **103**, 157–158 (1999).
- Carmeliet, P. Mechanisms of angiogenesis and arteriogenesis. *Nature Med.* **6**, 389–395 (2000).
- Yamaguchi, T. P., Dumont, D. J., Conlon, R. A., Breitman, M. L. & Rossant, J. Flk1, a flt-related receptor tyrosine kinase is an early marker for endothelial precursors. *Development* **118**, 489–498 (1993).
- Topouzis, S. & Majesky, M. W. Smooth muscle lineage diversity in the chick embryo—Two types of aortic smooth muscle cell differ in growth and receptor-mediated transcriptional responses to transforming growth factor- β . *Dev. Biol.* **178**, 430–445 (1996).
- Jiang, X., Rowitch, D. H., Soriano, P., McMahon, A. P. & Sucov, H. M. Fate of the mammalian cardiac neural crest. *Development* **127**, 1607–1616 (2000).
- Mikawa, T. & Gourdie, R. G. Pericardial mesoderm generates a population of coronary smooth muscle cells migrating into the heart along with in growth of the epicardial organ. *Dev. Biol.* **174**, 221–232 (1996).
- Shalaby, F., Rosant, J., Yamaguchi, T. P., Gertsenstein, M. & Wu, X. F. Failure of blood-island formation and vasculogenesis in Flk1-deficient mice. *Nature* **376**, 62–66 (1995).
- Eichmann, A. *et al.* Ligand-dependent of the endothelial and hematopoietic lineages from embryonic mesodermal cells expressing vascular endothelial growth factor 2. *Proc. Natl Acad. Sci. USA* **94**, 5141–5146 (1997).
- Hirashima, M., Kataoka, H., Nishikawa, S., Matsuyoshi, N. & Nishikawa, S. I. Maturation of embryonic stem cells into endothelial cells in an *in vitro* model of vasculogenesis. *Blood* **93**, 1253–1263 (1999).
- Nishikawa, S. I., Nishikawa, S., Hirashima, M., Matsuyoshi, N. & Kodama, H. Progressive lineage analysis by cell sorting and culture identifies FLK1⁺VE-cadherin⁺ cells at a diverging point of endothelial cells and hemopoietic lineages. *Development* **125**, 1747–1757 (1998).
- Ogawa, M. *et al.* Expression of $\alpha 4$ -integrin defines the earliest precursor of hematopoietic cell lineage diverged from endothelial cells. *Blood* **93**, 1168–1177 (1999).
- Ueda, M., Becker, A. E., Naruko, T. & Kojima, A. Smooth muscle cell de-differentiation is a fundamental change preceding wound healing after percutaneous transluminal coronary angioplasty in humans. *Coron. Artery Dis.* **6**, 71–81 (1995).
- Hellström, M., Kalin, M., Lindahl, P., Abramson, A. & Betsholtz, C. Role of PDGF-B and PDGFR- β in recruitment of vascular smooth muscle cells and pericytes during embryonic blood vessel formation in the mouse. *Development* **126**, 3047–3055 (1999).
- Soker, S., Takahashi, S., Miao, H. Q., Neufeld, G. & Klagsbrun, M. Neuropilin-1 is expressed by endothelial and tumor cells as an isoform-specific receptor for vascular endothelial growth factor. *Cell* **92**, 735–745 (1998).
- Lindahl, P., Johansson, B., Leveén, P. & Betsholtz, C. Pericyte loss and microaneurysm formation in PDGF-B-deficient mice. *Science* **277**, 242–245 (1997).
- Hirschi, K. K., Rohovsky, S. A., Beck, L. H., Smith, S. R. & D'Amore, P. A. Endothelial cells modulate the proliferation of mural cells precursors via platelet-derived growth factor-BB and heterotypic cell contact. *Circ. Res.* **84**, 298–305 (1999).
- Benjamin, L. E., Hemo, I. & Keshet, E. A plasticity window for blood vessel remodelling is defined by pericyte coverage of the preformed endothelial network and is regulated by PDGF-B and VEGF. *Development* **125**, 1591–1598 (1998).
- DeRuiter, M. C. *et al.* Embryonic endothelial cells transdifferentiate into mesenchymal cells expressing smooth muscle actin *in vivo* and *in vitro*. *Circ. Res.* **80**, 444–451 (1997).
- Hirschi, K. K., Rohovsky, S. A. & D'Amore, P. A. PDGF, TGF- β , and heterotypic cell-cell interactions mediate endothelial cell-induced recruitment of 10T1/2 cells and their differentiation to a

smooth muscle fate. *J. Cell. Biol.* **141**, 805–814 (1998).

- Cuevas, P. *et al.* Pericyte endothelial gap junctions in human cerebral capillaries. *Anat. Embryol.* **170**, 155–159 (1984).
- Choi, K., Kennedy, M., Kazarov, A., Papadimitriou, J. C. & Keller, G. A common precursor for hematopoietic and endothelial cells. *Development* **125**, 725–732 (1998).
- Takakura, N., Kodama, H., Nishikawa, S. & Nishikawa, S. I. Preferential proliferation of murine colony-forming units in culture in a chemically defined condition with a macrophage colony-stimulating factor-negative stromal cell clone. *J. Exp. Med.* **184**, 2301–2309 (1996).
- Shirayoshi, Y., Nose, A., Iwasaki, K. & Takeichi, M. N-linked oligosaccharides are not involved in the function of a cell-cell binding glycoprotein E-cadherin. *Cell Struct. Funct.* **11**, 245–252 (1986).
- Kataoka, H. *et al.* Expressions of PDGF-receptor alpha, c-kit, and FLK1 genes clustering in mouse chromosome 5 define distinct subsets of nascent mesodermal cells. *Dev. Growth Differ.* **39**, 729–740 (1997).
- Matsuyoshi, N. *et al.* *In vivo* evidence of the critical role of cadherin-5 in murine vascular integrity. *Proc. Assoc. Am. Physicians* **109**, 362–371 (1997).
- Yoshida, H. *et al.* IL-7 receptor α^+ CD3⁻ cells in the embryonic intestine induces the organizing center of Peyer's patches. *Int. Immunol.* **11**, 643–655 (1999).
- Isobe, S., Chen, S. T., Nakane, P. K. & Brown, W. R. Studies on translocation of immunoglobulins across intestinal epithelium. I. Improvements to study the peroxidase-labeled antibody method for application to study of human intestinal mucosa. *Acta Histochem. Cytochem.* **10**, 161–171 (1977).
- Yamamoto, T. *et al.* Repopulation of murine Kupffer cells after intravenous administration of liposome-encapsulated dichloromethylene diphosphonate. *Am. J. Pathol.* **149**, 1271–1286 (1996).

Supplementary information is available on Nature's World-Wide Web site (<http://www.nature.com>) or as paper copy from the London editorial office of Nature.

Acknowledgements

We thank M. J. Evans for CCE ES cells, N. Matsuyoshi for the hybridoma, A. Nagafuchi for antibodies, T. Kunisada for LacZ construct, R. Yu for critical reading of the manuscript, and many of our colleagues for suggestions and discussion. This work was supported by grants from the Ministry of Education, Science, Sports and Culture of Japan, the Ministry of Health and Welfare of Japan (S.I.N.), Japanese Society for the Promotion of Science "Research for the Future" Program (H.I., M.O. and S.I.N.), Japan Tobacco Foundation, Japan Hearth Foundation & Pfizer Pharmaceuticals Grant for Research on Coronary Artery Disease and Tanabe Medical Frontier Conference. J.Y. is a recipient of the Research Fellowship grant of the Japan Society for the Promotion of Science for Young Scientists.

Correspondence and requests for materials should be addressed to J.Y. (e-mail: juny@kuhp.kyoto-u.ac.jp).

Bidirectional control of airway responsiveness by endogenous cannabinoids

A. Calignano^{*}, I. Kátóná[†], F. Désarnaud[‡], A. Giuffrida[‡], G. La Rana^{*}, K. Mackie[§], T. F. Freund[†] & D. Piomelli[‡]

^{*} Department of Pharmacology, University of Naples, Naples 80131, Italy

[†] Institute of Experimental Medicine, Budapest 1450, Hungary

[‡] Department of Pharmacology, University of California, Irvine, California 92697-4625, USA

[§] Department of Anesthesiology, University of Washington, Seattle, Washington 98195-6540, USA

Smoking marijuana or administration of its main active constituent, Δ^9 -tetrahydrocannabinol (Δ^9 -THC), may exert potent dilating effects on human airways^{1–4}. But the physiological significance of this observation and its potential therapeutic value are obscured by the fact that some asthmatic patients respond to these compounds with a paradoxical bronchospasm^{3,5}. The mechanisms underlying these contrasting responses remain unresolved. Here we show that the endogenous cannabinoid anandamide exerts dual effects on bronchial responsiveness in rodents: it strongly inhibits bronchospasm and cough evoked by the chemical irritant, capsaicin, but causes bronchospasm when the constricting tone exerted by the vagus nerve is removed. Both effects are mediated through peripheral CB1 cannabinoid receptors found on axon terminals of airway nerves. Biochemical

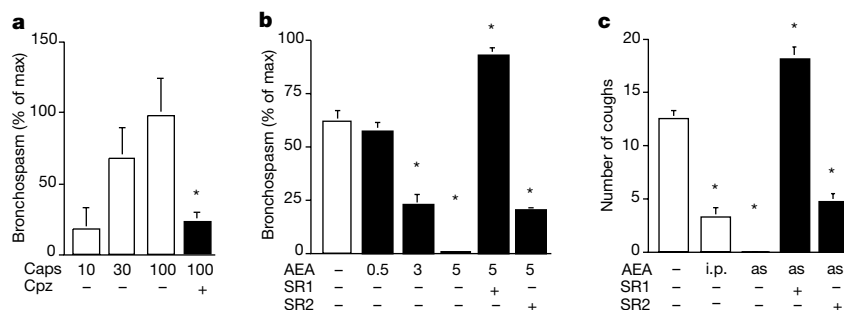


Figure 1 Anandamide inhibits bronchospasm and coughing in guinea-pigs by activating peripheral CB1 receptors. **a**, Constricting effect of capsaicin (Caps, μg per kg i.v.) on guinea pig bronchial smooth muscle and its antagonism by capsazepine (Cpz, 0.2 mg per kg i.v.). **b**, Inhibitory effects of anandamide (AEA, mg per kg i.v.) on capsaicin-evoked (30 μg per kg) bronchospasm in the absence or presence of the CB1 antagonist

SR141716A (SR1, 0.5 mg per kg i.v.) or the CB2 antagonist SR144528 (SR2, 0.3 mg per kg i.v.). **c**, Inhibition of capsaicin-evoked cough by anandamide in the absence or presence of SR141716A (0.5 mg per kg i.v.) or SR144528 (0.3 mg per kg i.v.). Asterisk, $P < 0.01$ ($n = 3$ for each condition).

analyses indicate that anandamide is synthesized in lung tissue on calcium-ion stimulation, suggesting that locally generated anandamide participates in the intrinsic control of airway responsiveness. In support of this conclusion, the CB1 antagonist SR141716A enhances capsaicin-evoked bronchospasm and cough. Our results may account for the contrasting bronchial actions of cannabis-like drugs in humans, and provide a framework for the development of more selective cannabinoid-based agents for the treatment of respiratory pathologies.

To explore the functional roles of the cannabinoid system in airway physiology, we investigated the effects of the endogenous cannabinoid, anandamide^{6,7}, on the responsiveness of bronchial smooth muscle. Administration of capsaicin, the pungent component of chilli pepper⁸, produces a potent bronchoconstriction in anaesthetized guinea pigs (Fig. 1a) or rats (in μg per animal, intratracheal: 10, $41 \pm 6\%$ of maximal bronchospasm; 30, $55 \pm 12\%$; 100, $81 \pm 19\%$; means \pm s.e.m., $n = 3$). This response, which has been extensively studied both in animals and humans, is thought to result from the activation of capsaicin (or ‘vanilloid’) receptors on sensory C-fibres⁹. Accordingly, the constricting effects of capsaicin were blocked by the vanilloid antagonist capsazepine (Fig. 1a). When administered systemically before capsaicin, anandamide produced a dose-dependent attenuation of bronchospasm in guinea-pigs (Fig. 1b) and rats (capsaicin, 10 μg per animal, intratracheal: $37.2 \pm 4.2\%$ of maximal bronchospasm; capsaicin after anandamide, 1 mg per kg intravenous (i.v.), $14 \pm 7\%$, $n = 3$). This effect was completely reversed by the selective CB1 cannabinoid antagonist SR141716A (ref. 10) but only slightly reduced with a maximal dose of the CB2 antagonist SR144528 (ref. 11) (Fig. 1b and data not shown). Palmitylethanolamide, a structural analogue of anandamide that inhibits nociception in mice, but does not interact with CB1 receptors¹², was ineffective at alleviating capsaicin-evoked bronchospasm (data not shown). When given as an aerosol to conscious guinea-pigs, capsaicin stimulates C-fibre activity in the upper respiratory tract and triggers coughing^{13,14}. Systemic or aerosolized anandamide reduced capsaicin-evoked coughing, an effect that was cancelled by CB1 receptor blockade (Fig. 1c).

Anandamide had no direct bronchomotor action, except at the highest dose tested (5 mg per kg), at which the compound elicited a small bronchoconstriction ($11.8 \pm 5.9\%$ of maximal; mean \pm s.e.m., $n = 5$). To investigate this response further, we examined the effects of anandamide in anesthetized rodents that were deprived of the bronchoconstricting tone conferred by the vagus nerve⁹. After vagotomy and atropine administration, which eliminate vagal influences, systemic application of anandamide produced a dose-dependent bronchoconstriction in guinea pigs (Fig. 2a) and rats (in mg per kg i.v.: 1, $0 \pm 0\%$ of maximal bronch-

ospasm; 3, $12 \pm 1.7\%$, 5, $18.3 \pm 1.2\%$; $n = 3$). Similar effects were observed when anandamide was injected into the guinea-pig bronchi through a tracheal catheter (Fig. 2b), or applied to isolated strips of guinea-pig lung parenchyma (Fig. 2c–e). The slow onset of the anandamide response in strips of guinea-pig lung is consistent with results obtained in other isolated tissues⁶; the low potency of anandamide in this preparation may be accounted for by limited tissue penetration and/or rapid inactivation. In agreement with this possibility, the anandamide transport inhibitor AM404 enhanced anandamide-evoked contractions in isolated strips of guinea-pig lung (anandamide, 50 μM , 0.336 ± 0.07 dyne mg^{-1} of tissue; anandamide plus AM404, 28 μM , 0.638 ± 0.06 dyne mg^{-1} of tissue; $P < 0.05$, $n = 6$). The CB1 antagonist SR141716A blocked

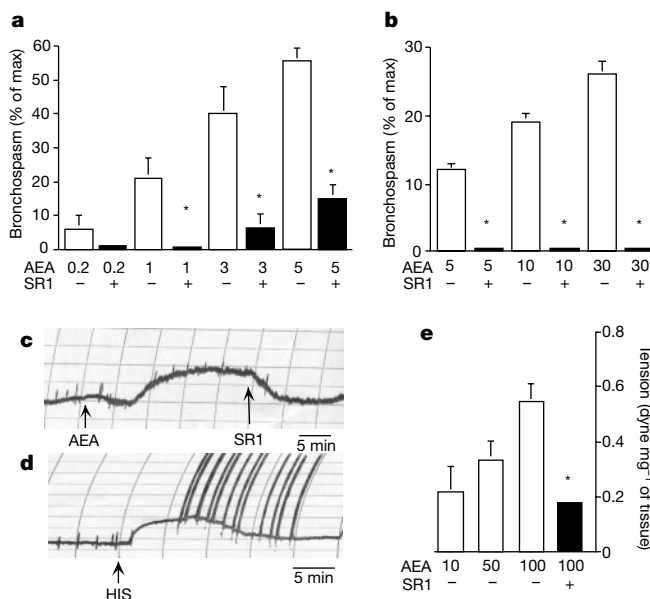


Figure 2 Anandamide causes bronchoconstriction in vagotomized, atropine-treated guinea pigs by activating peripheral CB1 receptors. **a**, Effects of anandamide (AEA, mg per kg i.v.) in the presence or absence of the CB1 antagonist SR141716A (SR1, 0.2 mg per kg i.v.) ($n = 6$ for each condition). **b**, Effects of anandamide (5–30 μg per animal, intratracheal) in the absence or presence of SR141716A (SR1, 0.3 mg per kg i.v.) ($n = 6$). **c**, Representative tracing illustrating the effect of anandamide (100 μM) on muscle tension in guinea pig parenchyma strips and its reversal by the CB1 antagonist SR141716A (1 μM). **d**, Response of the same lung strip to histamine (His, 10 μM). **e**, Contractions of lung parenchyma by anandamide (μM) and antagonism by SR141716A (1 μM) ($n = 6$). Asterisk, $P < 0.01$.

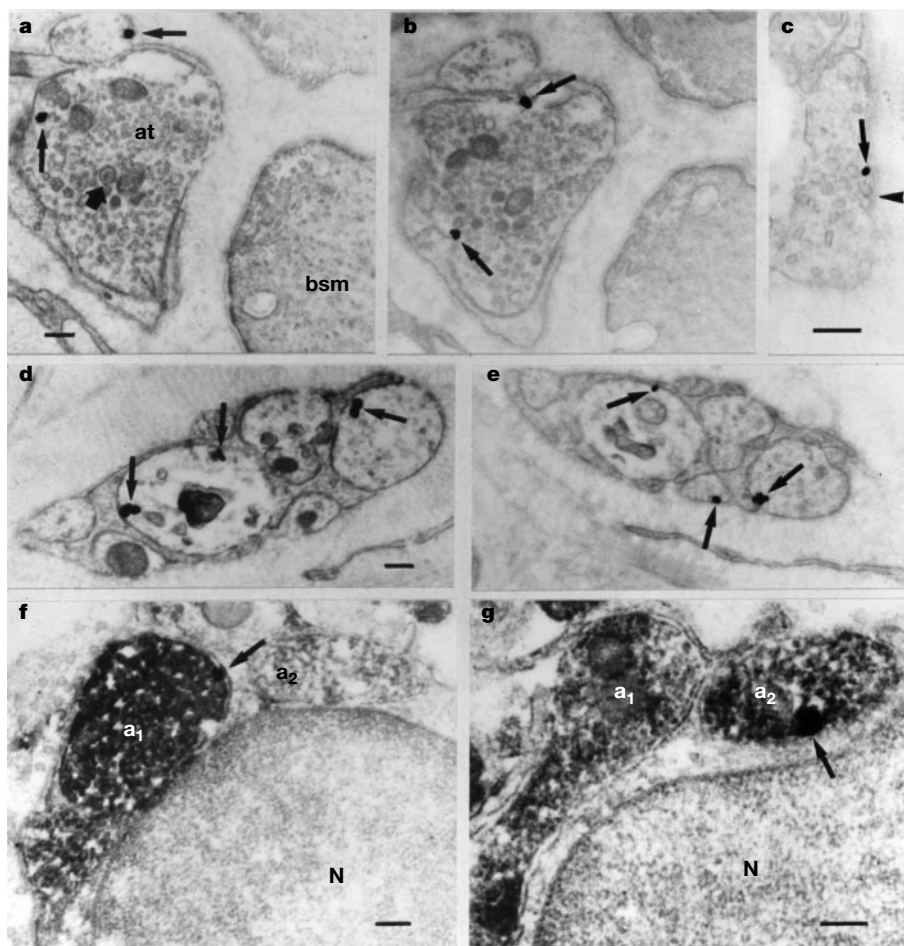


Figure 3 Localization of CB1 receptors on axon terminals and preterminal segments in rat lungs. **a, b**, CB1 receptor labelling is indicated by thin arrows on sections of bronchiole axon terminals. Axon terminals (at) containing small electron-translucent and large dense-core vesicles (thick arrow) are embedded in the collagen matrix and are surrounded by bronchial smooth muscle cells (bsm). **c**, CB1 receptor labelling close to

putative neurotransmitter release sites (arrowhead). **d, e**, Several axon terminals packed together into glial capsules in the adventitia. **f, g**, Co-localization of CB1 receptor and NPY. CB1 receptor labelling appears on axon terminal membranes (a_1 and a_2) displaying electron-dense NPY immunoreactivity. N, nucleus of a putative Schwann cell. Scale bars, 0.2 μm (scales in **b** and **e** are the same as in **a** and **d**, respectively).

anandamide bronchoconstriction *in vivo* and *in vitro* (Fig. 2a–e), whereas the CB2 antagonist SR144528 had no effect (data not shown). The cannabinoid agonist HU210 was also potent at eliciting guinea pig bronchial muscle constriction after tracheal administration (in μg per animal: 10.0 \pm 0.6% of maximal bronchoconstriction; 1, 30 \pm 1.2%; 10, 60 \pm 2.2%; 30, 100%; $n = 6$). Anandamide has been claimed to activate vanilloid receptors¹⁵. However, the vanilloid antagonist capsazepine had no effect on anandamide-evoked bronchoconstriction at a dose that completely prevented the capsaicin response (0.2 mg per kg *i.v.*) (data not shown). These results indicate that removing the vagal excitatory tone unmasked a bronchoconstricting activity of anandamide mediated through CB1 receptors.

The ability of anandamide to influence bronchial muscle contractility after local administration suggests that this compound may exert its effects by activating CB1 receptors located within the airways. To test this possibility, we examined the ultrastructural localization of CB1 receptors in rat lungs by electron microscopy, using an antibody directed against the intracellular carboxy terminus of the CB1 receptor protein. Immunogold staining revealed that CB1 receptors are present on nerve fibres distributed among bronchial and bronchiolar smooth muscle cells (Fig. 3a–c), or between the longitudinal and circular smooth muscle layers, where several axons are packed together into glial capsules (Fig. 3d, e). All bundles contained at least one CB1-receptor-

positive axon. Detailed evaluation (20 bundles consisting of 91 axons followed through at least 25 consecutive sections) revealed that 36% of the axons were labelled with the CB1 receptor antibody. The gold particles that labelled CB1 receptors were attached to the inner surface of the axon plasma membrane, either at the release site or in the preterminal segments. This is consistent with the fact that the antibody we used recognizes the intracellular C terminus of the CB1 receptor protein. Axon terminals bearing CB1 receptor immunoreactivity were in close proximity to smooth muscle cells (0.2–0.5 μm), and contained a large number of small agranular vesicles, along with few dense-core vesicles (Fig. 3a, b). In some cases, CB1 receptor immunoreactivity was adjacent to clusters of vesicles accumulated at the plasma membrane, which most probably represent neurotransmitter release sites (Fig. 3c). Next, to determine whether CB1 receptors are localized on noradrenaline-containing and/or non-noradrenaline-containing fibres, we used a combination of immunogold staining for CB1 receptors, and immunoperoxidase staining for neuropeptide Y (NPY), a co-transmitter in sympathetic neurons⁹. We found that 63% of NPY-bearing axons were also CB1-receptor-positive (Fig. 3f, g). Notably, however, extensive labelling was observed on many NPY-negative axons (data not shown), suggesting that both noradrenaline-containing and/or non-noradrenaline-containing nerves may express CB1 receptors.

The finding that CB1 receptors are found predominantly, if not

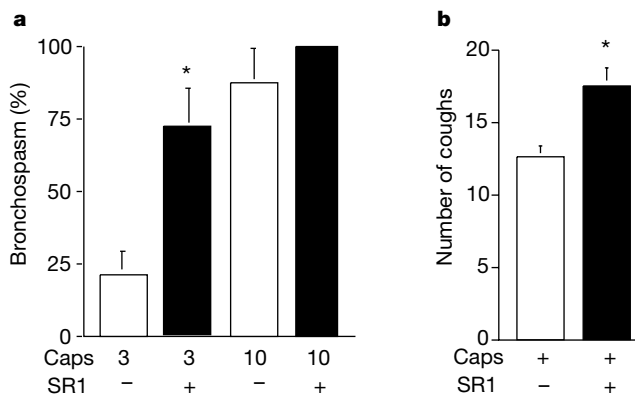


Figure 4 Intrinsic effects of the CB1 antagonist SR141716A on capsaicin-evoked bronchospasm and cough. **a**, Bronchoconstricting effects of capsaicin (μg per animal, intratracheal) in the absence or presence of the CB1 antagonist SR141716A (0.2 mg per kg i.v.). **b**, Tussigenic effects of capsaicin (0.3 mM, 4-min aerosol) in the absence or presence of SR141716A (0.2 mg per kg i.v.) ($n = 6$ for each condition). Asterisk, $P < 0.05$.

exclusively, on axon terminals of airway nerves indicates that anandamide may regulate bronchial smooth muscle tone through a prejunctional mechanism. Inhibition of excitatory neurotransmission in the airways may provide a parsimonious explanation for the ability of anandamide to oppose capsaicin-evoked bronchospasm and cough. This interpretation is further supported by the ability of anandamide and other cannabinoid agonists to inhibit neurotransmitter release in both peripheral tissues^{16–18} and the central nervous system¹⁹. The mechanism underlying the constricting actions of anandamide in animals lacking acetylcholine-mediated control is currently unknown. One possibility, which is consistent with the co-localization of CB1 receptors with NPY, is that anandamide inhibits the release of a bronchodilating mediator. Alternatively, anandamide may interact with CB1 receptors on smooth muscle. Our failure to detect CB1 receptor immunoreactivity in lung smooth muscle may have been caused by insufficient sensitivity of our technique, or by the presence in smooth muscle of a receptor variant that is not recognized by our antibody. Interestingly, northern blot analyses suggest that alveolar type II cells in the lung may express two different CB1 receptor messenger RNA species²⁰.

To test the possibility that endogenous cannabinoids regulate airway responsiveness, we determined the intrinsic effects of CB1 and CB2 antagonists on bronchospasm and cough in guinea-pigs. CB1 receptor blockade with SR141716A had no bronchomotor consequences *per se*, but significantly enhanced the bronchoconstriction and coughing evoked by capsaicin administered through a tracheal catheter (Fig. 4a, b), even in the presence of anandamide (Fig. 1b, c). This response did not depend on the capsaicin administration route, as it was also seen after i.v. injection of the drug (30 mg per kg capsaicin alone, $55.3 \pm 8.2\%$ of maximal bronchospasm; capsaicin after SR141716 (0.5 mg per kg i.v.), $92.3 \pm 3.4\%$; $P < 0.05$, $n = 3$). The CB2 antagonist SR144528 had no effect on capsaicin-induced bronchoconstriction and cough (data not shown).

Although the bronchomotor actions of the CB1 antagonist may be accounted for by its inverse agonist properties²¹, evidence suggests that this drug acted by opposing an ongoing cannabinoid modulation. First, the lack of effect seen with the CB1 antagonist in the absence of capsaicin is incompatible with an inverse agonist behaviour. Second, analyses by high-performance liquid chromatography (HPLC) coupled to positive-ionization electrospray mass spectrometry (MS) revealed that anandamide is synthesized in rat lung tissue through a Ca^{2+} -ion-activated mechanism (Fig. 5). Rat

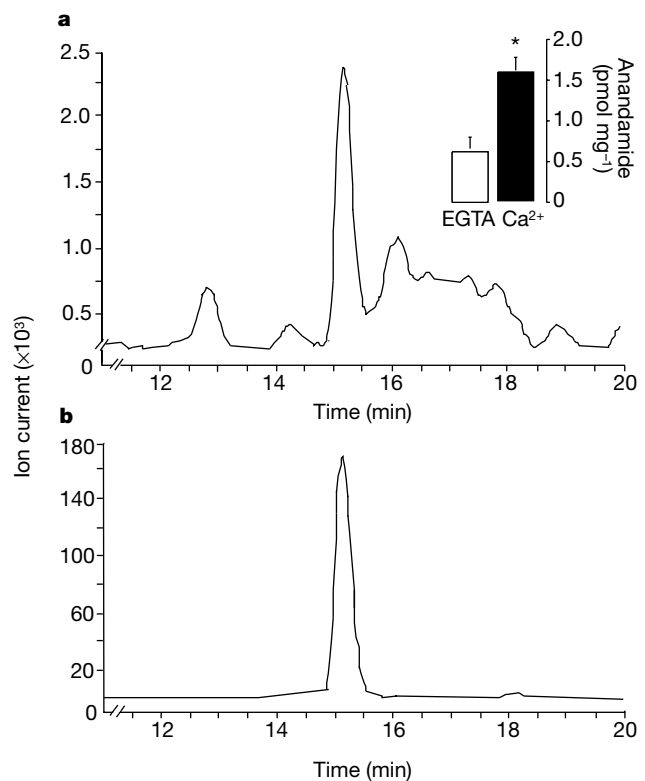


Figure 5 Ca^{2+} -dependent biosynthesis of anandamide in rat lung tissue. Representative HPLC/MS tracings for selected ions characteristic of endogenous anandamide (**a**, mass-to-charge ratio $m/z = 370$, an adduct with Na^+ , $[\text{M} + \text{Na}]^+$) and synthetic [²H₄]anandamide (**b**, $m/z = 374$, $[\text{M} + \text{Na}]^+$), which was added to the samples as an internal standard. The inset in **a** illustrates the effects of EGTA (1 mM) or Ca^{2+} (3 mM) on anandamide biosynthesis in rat lung membranes. Ca^{2+} significantly stimulated anandamide formation (mean \pm s.e.m.; asterisk, $P < 0.05$, $n = 4$).

lung membranes produced on average 0.6 ± 0.2 pmol of anandamide per mg of protein in the presence of the Ca^{2+} chelator EGTA (1 mM); and 1.6 ± 0.2 pmol of anandamide per mg of protein in the presence of Ca^{2+} (3 mM) (mean \pm s.e.m., $n = 4$; $P < 0.05$ between EGTA and Ca^{2+} ; Student's *t*-test) (Fig. 5, inset). Guinea-pig lung membranes produced 0.9 ± 0.3 pmol of anandamide per mg of protein in the presence of EGTA; and 8.8 ± 1.2 pmol of anandamide per mg of protein in the presence of Ca^{2+} ($n = 4$; $P < 0.0001$; Student's *t*-test).

Anandamide is thought to originate from the enzymatic cleavage of *N*-arachidonyl phosphatidylethanolamine (NAPE), the biosynthesis of which is catalysed by a Ca^{2+} -dependent *N*-acyltransferase activity^{7,22,23}. Using negative ionization electrospray HPLC/MS, we identified two molecular species of NAPE in lipid extracts of rat lung membranes: alk-1-palmitoonyl-2-arachidonyl-*sn*-glycerophosphoethanolamine-*N*-arachidonyl (NAPE 1; Fig. 6a) and alk-1-stearyl-2-arachidonyl-*sn*-glycerophosphoethanolamine-*N*-arachidonyl (NAPE 2; Fig. 6a). Identifications were based (1) on the occurrence of deprotonated molecules of appropriate mass (NAPE 1: mass-to-charge ratio (m/z) 1009; and NAPE 2, m/z 1039); and (2) on the chromatographic behaviour of these components, which was similar to that of synthetic NAPE (Fig. 6b; see Methods). NAPE 1 and NAPE 2 were synthesized by rat lung membranes in a Ca^{2+} -dependent manner. The membranes produced 1.5 ± 0.02 pmol of NAPE 1 and undetectable levels in NAPE 2 when incubated with EGTA (1 mM); and 4.4 ± 0.5 pmol of NAPE 1 and 3.1 ± 0.6 pmol of NAPE 2 when incubated with Ca^{2+} (3 mM) ($n = 4$; $P < 0.05$ between EGTA and Ca^{2+}) (Fig. 6b, insets). Guinea pig lung membranes also produced NAPE 1 and NAPE 2 in a Ca^{2+} -dependent

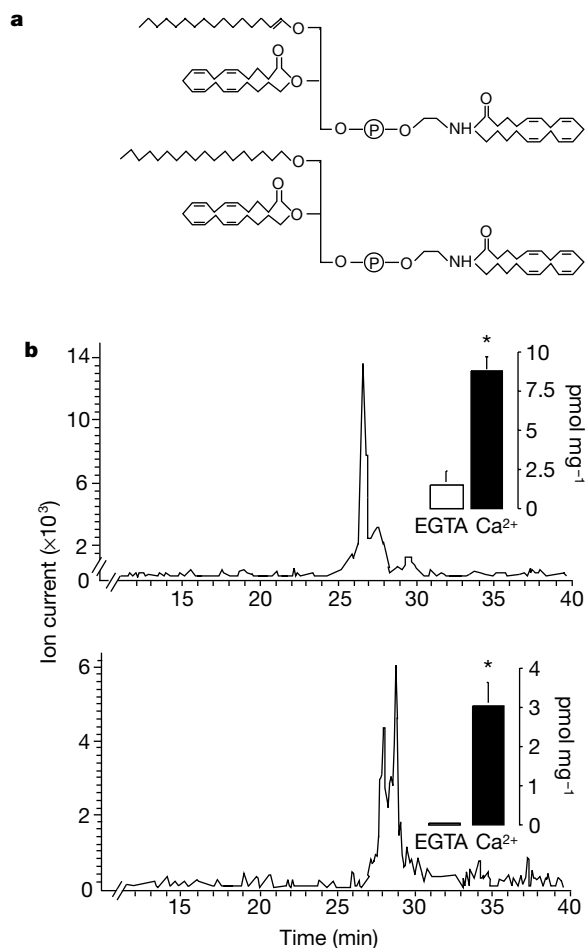


Figure 6 Ca²⁺-dependent biosynthesis of anandamide precursors in rat lung. **a**, Structures of alk-1-palmitoeyl-2-arachidonyl-*sn*-glycero-phosphoethanolamine-*N*-arachidonyl (top panel, NAPE 1) and alk-1-stearyl-2-arachidonyl-*sn*-glycero-phosphoethanolamine-*N*-arachidonyl (bottom panel, NAPE 2), two anandamide precursors. **b**, Representative HPLC/MS tracings for selected ions characteristic of NAPE 1 (top panel, *m/z* = 1009, deprotonated molecule, [M - H]⁻) and NAPE 2 (bottom panel, *m/z* = 1039, [M - H]⁻). The insets show that biosynthesis of NAPE 1 (top panel) and NAPE 2 (bottom panel) was significantly stimulated by Ca²⁺ (3 mM) (mean ± s.e.m.; asterisk, *P* < 0.05, *n* = 4).

manner (data not shown). The presence in rodent lungs of a Ca²⁺-activated mechanism for the biosynthesis of anandamide and its phospholipid precursor supports a role for this endogenous cannabinoid in airway modulation.

Our results indicate that activation of CB1 receptors by locally released anandamide may participate in the control of bronchial contractility. How anandamide exerts such control may depend, however, on the state of the bronchial muscle. When the muscle is contracted, as during capsaicin-evoked bronchospasm, anandamide may counteract this contraction, possibly by inhibiting the prejunctional release of excitatory neurotransmitters and neuropeptides. In contrast, when the smooth muscle is relaxed, as seen after removal of the constricting influence of the vagus nerve, anandamide may cause bronchoconstriction. These state-dependent effects may account for the variable bronchomotor actions of acutely administered cannabis-like agents in humans, and might contribute to the long-term toxicity associated with cannabis smoking²⁴. Furthermore, the existence of an intrinsic cannabis-mediated control of airway function may open perspectives for the development of new antitussive and anti-asthmatic agents. For example, drugs targeting the mechanisms of anandamide

inactivation²⁵ may exert more selective pharmacological effects on bronchial responsiveness than those elicited by direct-acting CB1 agonists. □

Methods

Chemicals

Anandamide and [²H]anandamide were synthesized following standard procedures; 1-palmityl-2-oleyl-*sn*-glycero-phosphoethanolamine-*N*-arachidonyl and 1,2-dioleoyl-*sn*-glycero-phosphoethanolamine-*N*-oleyl were purchased from avanti Polar Lipids (Alabaster, AL); SR144528 (*N*-[(1*S*)-endo-1,3,3-trimethyl bicyclo [2.2.1] heptan-2-yl]-5-(4-chloro-3-methylphenyl)-1-(4-methylbenzyl)-pyrazole-3-carboxamide) was a generous gift from Sanofi Recherche (Montpellier, France); SR141716A ([*N*-(piperidin-1-yl)-5-(4-chlorophenyl)-1-(2,4-dichlorophenyl)-4-methyl-1*H*-pyrazole-3-carboxamide-HCl) was provided by RBI (Natick, MA) as part of the Chemical Synthesis Program of the NIMH (N01MH30003); all other drugs were from Tocris (Ballwin, MO) or Sigma (Saint Louis, MO). The drugs were dissolved in dimethylsulphoxide (DMSO), and administered in physiological saline containing 10% DMSO.

Biological assays

For bronchospasm, we anaesthetized Dunkin-Hartley guinea-pigs (Charles-River, weighing 200–400 g) or Wistar rats (Charles-River, weighing 200–300 g) with pentobarbital (40 mg per kg intraperitoneal (i.p.)) and fentanyl (25 µg per kg intramuscular), catheterized the trachea and carotid artery to measure airway obstruction and systemic blood pressure, and catheterized the jugular vein to administer drugs. Pancuronium bromide (4 mg per kg i.v.) was administered to prevent spontaneous breathing. The animals were ventilated with room air using a rodent ventilator (U. Basile, Comerio, Italy) run at 60 strokes min⁻¹; stroke volume was 3–7 ml. Airway resistance was measured by using a differential pressure transducer (U. Basile) connected by the side-arm of the tracheal catheter to a bronchospasm transducer. Bronchospasm was expressed as a per cent of the maximal response, which was determined by clamping the tracheal catheter before and after each experiment. Drugs were dissolved in saline containing 10% DMSO, and injected through the jugular vein; responses were evaluated at their peak. Arterial blood pressure was measured continuously with a pressure transducer connected to a recorder (U. Basile). To abolish vagal influences on bronchial musculature, in some experiments we bilaterally transected the vagus nerves and administered atropine sulphate (2 mg per kg i.v.). Anandamide was administered 15 min before capsaicin; the antagonists were given 15 min before anandamide.

For coughing, we individually exposed conscious guinea-pigs to aerosolized capsaicin (0.3 mM) for 4 min while recording coughs by using a microphone placed in the exposure chamber²⁶. Each animal was treated only once with capsaicin. Anandamide was administered either systemically (i.p. 30 min before capsaicin) or locally (by aerosol, 10 mg per ml, 15 min before capsaicin). Aerosols were prepared with an Air Lister Basic apparatus (Hatü, Italy), regulated at an emission flow rate of 6 l min⁻¹. For isolated lung strips, guinea-pig parenchymal strips were prepared essentially as described²⁷. The strips were placed in 10-ml organ baths containing Krebs' buffer (in mM: NaCl, 118; KCl, 4; K₂HPO₄, 1.2; MgSO₄, 1.2; CaCl₂, 2.5; NaHCO₃, 25.0; glucose, 11.2; supplemented with 7 µM atropine sulphate and 15 µM indomethacin) at 37 °C and aerated with an oxygen/carbon dioxide mixture (95/5%). Muscle contractions were recorded with an isometric force transducer (U. Basile) and are expressed in dyne per mg of fresh tissue.

Electron microscopy

The lungs were removed from three rats perfused with a phosphate-buffered (0.1 M) fixative containing 4% paraformaldehyde, 0.2% picric acid and 0.05% glutaraldehyde, and were further fixed for 24 h. We carried out immunohistochemical analyses as described¹⁹. Rabbit C-terminal anti-CB1 and anti-NPY antibodies were used at 1:5,000 and 1:20,000 dilution, respectively. The specificity of the NPY antibody was reported previously²⁸; the specificity of the CB1 antibody has been verified in several ways, including staining of CB1 knockout mice, and will be detailed elsewhere (N. Hájos, I. K., C. Ledent, K. M. and T. F. F., manuscript in preparation).

Membrane preparation and lipid extraction

Lung particulate fractions were prepared as described²⁹. We carried out incubations for 1 h at 37 °C in Tris buffer (50 mM, pH 7.4) containing CaCl₂ (3 mM) or EGTA (1 mM) and 2 mg ml⁻¹ of membrane protein. Reactions were stopped by adding cold methanol, and the lipids were extracted with chloroform. Before HPLC/MS analysis, we fractionated anandamide and NAPE by silica gel column chromatography²³.

HPLC/MS

Anandamide was identified and quantified by reversed-phase HPLC coupled to positive ionization electrospray MS, by using an isotope-dilution method as described³⁰. We purified NAPE species by reversed-phase HPLC on a C₁₈ Bondapak column (300 × 3.9 mm internal diameter 5 µm) (Waters) maintained at 20 °C and interfaced with an Agilent HP1100 model mass spectrometer. HPLC conditions consisted of a linear gradient of methanol in water (from 75 to 100% methanol in 30 min) with a flow rate of 1 ml min⁻¹. Under these conditions, different NAPE species were eluted from the column as a group of peaks at retention times comprising 27–29 min. MS analyses were performed with the electrospray ion source set in the negative ionization mode; the V_{cap} set at 5 kV; and the fragmentor voltage set at 200 V. Nitrogen was used as a drying gas at a flow rate of

12 l min⁻¹. The drying gas temperature was set at 350 °C, and the nebulizer pressure at 30 PSI. For quantitative purposes, we extracted diagnostic ions (deprotonated molecules, [M - H]⁻) from full scan data and quantified them by comparison with an external standard (1-palmityl-2-oleyl-*sn*-glycero-phosphoethanolamine-*N*-arachidonyl, Avanti Polar Lipids). NAPE 2 was eluted from the column as a doublet, and the areas under both peaks were combined for quantification.

Data analysis

Results are expressed as means ± s.e.m. The significance of differences among groups was evaluated using Student's *t*-test or analysis of variance followed by Dunnett's test.

Received 8 June; accepted 7 August 2000.

1. Vachon, L., Fitzgerald, M. X., Solliday, N. H., Gould, I. A. & Gaensler, E. A. Single-dose effects of marijuana smoke. Bronchial dynamics and respiratory-center sensitivity in normal subjects. *New Engl. J. Med.* **288**, 985–989 (1973).
2. Tashkin, D. P., Shapiro, B. J., Lee, Y. E. & Harper, C. E. Effects of smoked marijuana in experimentally induced asthma. *Am. Rev. Respir. Dis.* **112**, 377–386 (1975).
3. Tashkin, D. P. *et al.* Bronchial effects of aerosolized delta 9-tetrahydrocannabinol in healthy and asthmatic subjects. *Am. Rev. Respir. Dis.* **115**, 57–65 (1977).
4. Iversen, L. L. *The Science of Marijuana* (Oxford Univ. Press, Oxford, 2000).
5. Abboud, R. T. & Sanders, H. D. Effect of oral administration of delta-9-tetrahydrocannabinol on airway mechanics in normal and asthmatic subjects. *Chest* **70**, 480–485 (1976).
6. Devane, W. *et al.* Isolation and structure of a brain constituent that binds to the cannabinoid receptor. *Science* **258**, 1946–1949 (1992).
7. Di Marzo, V. *et al.* Formation and inactivation of endogenous cannabinoid anandamide in central neurons. *Nature* **372**, 686–691 (1994).
8. Szallasi, A. & Blumberg, P. M. Vanilloid (Capsaicin) receptors and mechanisms. *Pharmacol. Rev.* **51**, 159–212 (1999).
9. Barnes, P. J. Modulation of neurotransmission in airways. *Physiol. Rev.* **72**, 699–729 (1992).
10. Rinaldi-Carmona, M. *et al.* SR141716A, a potent and selective antagonist of the brain cannabinoid receptor. *FEBS Lett.* **350**, 240–244 (1994).
11. Rinaldi-Carmona, M. *et al.* SR144528, the first potent and selective antagonist of the CB2 cannabinoid receptor. *J. Pharmacol. Exp. Ther.* **284**, 644–650 (1998).
12. Calignano, A., La Rana, G., Giuffrida, A. & Piomelli, D. Control of pain initiation by endogenous cannabinoids. *Nature* **394**, 277–281 (1998).
13. Karlsson, J. -A. & Fuller, R. W. Pharmacological regulation of the cough reflex—from experimental models to antitussive effects in man. *Pulmonary Pharmacol. Ther.* **12**, 215–228 (1999).
14. Widdicombe, J. G. Afferent receptors in the airways and cough. *Respir. Physiol.* **114**, 5–15 (1998).
15. Zygmunt, P. M., Julius, L., Di Marzo, V. & Hogestatt, E. D. Anandamide—the other side of the coin. *Trends Pharmacol. Sci.* **21**, 43–44 (2000).
16. Ishac, E. J. *et al.* Inhibition of exocytotic noradrenaline release by presynaptic cannabinoid CB1 receptors on peripheral sympathetic nerves. *Br. J. Pharmacol.* **118**, 2023–2028 (1996).
17. Coutts, A. A., Pertwee, R. G., Fernando, S. R. & Nash, J. E. Inhibition by cannabinoid receptor agonists of acetylcholine release from guinea-pig myenteric plexus. *Br. J. Pharmacol.* **121**, 1557–1566 (1997).
18. Richardson, J. D., Kilo, S. & Hargreaves, K. M. Cannabinoids reduce hyperalgesia and inflammation via interaction with peripheral CB1 receptors. *Pain* **75**, 111–119 (1998).
19. Katona, I. *et al.* Presynaptically located CB1 cannabinoid receptors regulate GABA release from axon terminals of specific hippocampal interneurons. *J. Neurosci.* **19**, 4544–4558 (1999).
20. Rice, W., Shannon, J. M., Burton, F. & Fiedeldej, D. Expression of a brain-type cannabinoid receptor (CB1) in alveolar type II cells in the lung: regulation by hydrocortisone. *Eur. J. Pharmacol.* **327**, 227–232 (1997).
21. Landsman, R. S., Burke, T. H., Consroe, P., Roeske, W. R. & Yamamura, H. I. SR141716A is an inverse agonist at the human cannabinoid CB1 receptor. *Eur. J. Pharmacol.* **334**, R1–R2 (1997).
22. Sugiura, T. *et al.* Transacylase-mediated and phosphodiesterase-mediated synthesis of *N*-arachidonoylethanolamine, an endogenous cannabinoid-receptor ligand, in rat brain microsomes. *Eur. J. Biochem.* **240**, 53–62 (1996).
23. Cadas, H., di Tomaso, E. & Piomelli, D. Occurrence and biosynthesis of endogenous cannabinoid precursor, *N*-arachidonyl phosphatidylethanolamine, in rat brain. *J. Neurosci.* **17**, 1226–1242 (1997).
24. Van Hoozen, B. E. & Cross, C. E. Marijuana. Respiratory tract effects. *Clin. Rev. Allergy Immunol.* **15**, 243–269 (1997).
25. Piomelli, D., Giuffrida, A., Calignano, A. & Rodriguez de Fonseca, F. The endocannabinoid system as a target for therapeutic drugs. *Trends Pharmacol. Sci.* **21**, 218–224 (2000).
26. Bolster, D. C., Del Prado, M., O'Reilly, S., Mingo, G. & Hey, J. A. Evan's blue dye blocks capsaicin-induced cough and bronchospasm in the guinea pig. *Eur. J. Pharmacol.* **276**, R1–R3 (1995).
27. Samhoun, M. N. & Piper, P. J. The combined use of isolated strips of guinea-pig lung parenchyma and ileum as a sensitive and selective bioassay for leukotriene B₄. *Prostaglandins* **27**, 711–724 (1984).
28. Csiffary, A., Gorcs, T. J. & Palkovits, M. Neuropeptide Y innervation of ACTH-immunoreactive neurons in the arcuate nucleus of rats: a correlated light and electron microscopic double immunolabeling study. *Brain Res.* **506**, 215–222 (1990).
29. Désarnaud, F., Cadas, H. & Piomelli, D. Anandamide amidohydrolase activity in rat brain microsomes: Identification and partial characterization. *J. Biol. Chem.* **270**, 6030–6035 (1995).
30. Giuffrida, A., Rodriguez de Fonseca, F. & Piomelli, D. Quantification of bioactive acylethanolamides in rat plasma by electrospray mass spectrometry. *Anal. Biochem.* **280**, 87–93 (2000).

Acknowledgements

We thank S. Chen, M. Elefante, G. Fabozzi, G. Goda, E. Oswald and R. Russo for excellent experimental assistance; T. Dinh, H. Kim and F. Nava for reading the manuscript critically; and B. Vigh for discussion. This research was supported from the National Institute of Drug Abuse (D.P. and K.M.), by the Howard Hughes Medical Institute and OTKA (T.F.), and by MURST (A.C.).

Correspondence and requests for materials should be addressed to D.P. (e-mail: piomelli@uci.edu).

.....
Identification of genes that modify ataxin-1-induced neurodegeneration

Pedro Fernandez-Funez*†, Maria Laura Nino-Rosales*†, Beatrice de Gouyon*, Wei-Chi She*‡, James M. Luchak*, Pedro Martinez*, Enrique Turiegano§, Jonathan Benito§, Maria Capovilla*, Pamela J. Skinner||, Alanna McCall*, Inmaculada Canal§, Harry T. Orr||, Huda Y. Zoghbi*‡§# & Juan Botas*‡

* Department of Molecular and Human Genetics, † Department of Pediatrics, ‡ Program in Developmental Biology, and # Howard Hughes Medical Institute, Baylor College of Medicine, Houston, Texas 77030, USA
 § Departamento de Biología, Universidad Autónoma de Madrid, 28049 Madrid, Spain
 || Institute of Human Genetics, University of Minnesota, Minneapolis, Minnesota 55455, USA
 † These authors contributed equally to this work

.....
A growing number of human neurodegenerative diseases result from the expansion of a glutamine repeat in the protein that causes the disease¹. Spinocerebellar ataxia type 1 (SCA1) is one such disease—caused by expansion of a polyglutamine tract in the protein ataxin-1. To elucidate the genetic pathways and molecular mechanisms underlying neuronal degeneration in this group of diseases, we have created a model system for SCA1 by expressing the full-length human SCA1 gene in *Drosophila*. Here we show that high levels of wild-type ataxin-1 can cause degenerative phenotypes similar to those caused by the expanded protein. We conducted genetic screens to identify genes that modify SCA1-induced neurodegeneration. Several modifiers highlight the role of protein folding and protein clearance in the development of SCA1. Furthermore, new mechanisms of polyglutamine pathogenesis were revealed by the discovery of modifiers that are involved in RNA processing, transcriptional regulation and cellular detoxification. These findings may be relevant to the treatment of polyglutamine diseases and, perhaps, to other neurodegenerative diseases, such as Alzheimer's and Parkinson's disease.

Drosophila provides a flexible and powerful model to study neurodegenerative diseases. Using the GAL4/UAS system², we can control the level of transgene expression and direct expression to different cell types or even to specific neurons. Large-scale genetic screens allow us to identify the genes and pathways involved in pathogenesis. Because most of the genetic pathways involved in normal development and disease conditions are conserved between *Drosophila* and mammals, mechanisms of neuronal degeneration in *Drosophila* may prove relevant to neurodegeneration in humans. *Drosophila* models using polyglutamine or truncated polypeptides of ataxin-3 and huntingtin, for example, show the characteristic progressive neural degeneration and pathology^{3–6}, and overproduction of the Hsp70 and Hsp40 molecular chaperones suppresses polyglutamine-induced neurotoxicity^{3,5}.

Because polyglutamine peptides tend to be more toxic than the full-length proteins and do not elicit the cell-type-specific neurodegeneration characteristic of these diseases⁷, their activities might be distinct from those of the full-length proteins. Therefore, we generated transgenic flies expressing full-length ataxin-1 using the GAL4/UAS system. We cloned two human SCA1 complementary DNAs, differing in the size of their polyglutamine repeat tracts, into the *Drosophila* transformation vector pUAST. These constructs encoded ataxin-1 30Q (a wild-type human isoform) and ataxin-1 82Q (an expanded isoform) (Fig. 1). Six 82Q and four 30Q lines were generated.

We directed SCA1 expression to the eye retina using the *gmr*-GAL4 driver⁸ and estimated ataxin-1 levels in all transgenic lines by